Journal of Power Sources 189 (2009) 798–801

Contents lists available at ScienceDirect

Journal of Power Sources

journal homepage: www.elsevier.com/locate/jpowsour

Short communication

First-principles study on lithium removal from Li_2MnO_3

Yukinori Koyama [a,*], Isao Tanaka [a], Miki Nagao [b], Ryoji Kanno [b]

[a] Department of Materials Science and Engineering, Kyoto University, Yoshida, Sakyo, Kyoto 606-8501, Japan
[b] Department of Electronic Chemistry, Tokyo Institute of Technology, Nagatsuda, Midori, Yokohama 226-8502, Japan

ARTICLE INFO

Article history:
Received 20 June 2008
Accepted 24 July 2008
Available online 3 August 2008

Keywords:
First-principles calculation
Lithium manganese oxide
Crystallographic structure
Redox potential
Charge compensation

ABSTRACT

A systematic first-principles calculation based on density functional theory is carried out to discuss the redox mechanism of Li_2MnO_3. The lattices of structural models having *C*2/*m*- and *C*2/*c*-type stacking sequences can be regarded as hexagonal, while their symmetry is monoclinic. Different stacking sequences of $[Mn_{2/3}Li_{1/3}]$ layers do not cause differences in the energy or crystallographic structure, suggesting a disordered stacking sequence. A calculation for $Li_{2-x}MnO_3$ assuming topotactic lithium removal indicates that lithium removal can occur at a potential of about 4.6 V with a wide potential plateau. The electronic structure of $Li_{2-x}MnO_3$ shows that the manganese ions remain in the charge state of Mn^{4+} and the charge of the removed lithium ions is compensated by the oxidation of oxygen.

1. Introduction

Li_2MnO_3 has a layered structure analogous to that of α-$NaFeO_2$. Its chemical formula can be described as $Li[Mn_{2/3}Li_{1/3}]O_2$ in the conventional notation. Because of the similarity of the crystallographic structure, solid solutions of Li_2MnO_3 and lithium transition-metal oxides have been studied for use as positive electrodes of lithium batteries [1–10]. Li_2MnO_3 and its derivatives exhibit a large rechargeable capacity of more than 200 mA h g^{-1}, corresponding to 0.87 Li ions per formula unit of Li_2MnO_3. Characteristic potential profiles are observed in the first charge–discharge cycle; the potential curve has a flat and wide plateau at ~4.5 V in the first charging, while it becomes sloping in the following discharging. Mn^{4+} has, however, been considered as inert in electrochemical reactions. To explain the electrochemical activity of Li_2MnO_3 and its derivatives, several mechanisms for the first charging have been proposed:

(a) Oxidation of other transition-metal elements.
(b) Oxidation of Mn^{3+} associated with oxygen deficiency.
(c) Removal of lithium accompanied by oxygen loss.
(d) Oxidation of electrolyte and exchange of H^+ for Li^+.

In solid solutions, other transition-metal elements are likely to contribute to the redox reaction. However, Li_2MnO_3 itself also exhibits a large rechargeable capacity [6,7,9]. Thus, the redox of the other elements is not essential. Pasero et al. reported the oxygen deficiency of Li_2MnO_3, leading to the formation of Mn^{3+} to balance the charge [10]. However, the amount of oxygen deficiency reported was at most 1% and the average oxidation state of the Mn ions was more than 3.94. Hence, the oxygen deficiency is not the dominant cause of the large rechargeable capacity. Lu and Dahn suggested that both Li and O atoms were simultaneously removed during the first charging of $Li[Ni_xLi_{(1/3-2x/3)}Mn_{(2/3-x/3)}]O_2$ in addition to the oxidation of Ni^{2+} to Ni^{4+} [5]. Kim et al. suggested that the removal of lithium was accompanied by oxygen loss during the first charging [8], and they proposed an electrochemical process for the lithium removal accompanied by the removal of electrons from the oxygen 2p band, immediately followed by chemical reaction resulting in the oxygen loss. Robertson and Bruce reported a charge capacity of more than 300 mA h g^{-1} at 55 °C [7]. They proposed that the charging occurred by the oxidation of the nonaqueous electrolyte and that generated protons were exchanged for Li ions in Li_2MnO_3. They also proposed the removal of lithium accompanied by oxygen loss for charging at 30 °C, at which the charge capacity was markedly smaller. The redox mechanism of Li_2MnO_3 and its derivatives is still under debate and further investigation is necessary from various points of view. First-principles calculation based on density functional theory has become a powerful technique even in the field of lithium batteries. It is capable not only of illustrating the electronic structure but also of predicting many properties [11–15]. For instance, the redox potential can be estimated within an error of 0.2 V without the use of experimental parameters [15]. In this work, a systematic first-principles calculation has been carried out for Li_2MnO_3, focusing on the lithium removal from an energetic point of view.

* Corresponding author. Tel.: +81 75 753 5435; fax: +81 75 753 5447.
E-mail address: y.koyama@at7.ecs.kyoto-u.ac.jp (Y. Koyama).

0378-7753/$ – see front matter © 2008 Elsevier B.V. All rights reserved.
doi:10.1016/j.jpowsour.2008.07.073

2. Calculation

The generalized gradient approximation (GGA) [16] was applied to density functional theory with the so-called +U correlation [17] for Mn-3d states. The U parameter used was 5.0 eV, which was theoretically estimated for Mn^{4+} in spinel-type MnO_2 [15]. Spin-polarization was taken into account along with the ferromagnetic arrangement of spins in the $[Mn_{2/3}Li_{1/3}]$ layers. The plane-wave-basis projector augmented wave (PAW) method [18–21] was used. The radius cutoffs of the PAW potential were 1.08, 1.32, and 0.90 Å for Li, Mn, and O, respectively. A plane-wave cutoff energy of 400 eV was used. Integration in the Brillouin zone was performed on the basis of the Monkhorst–Pack scheme [22] using a k-point mesh with an interval of 0.05 Å^{-1} in each primitive lattice vector of the reciprocal space. Lattice constants and internal atomic positions were optimized until the residual forces and stresses became less than 10^{-3} eV Å^{-1} and 1 MPa, respectively. The structural models used are explained in the following sections.

3. Results and discussion

3.1. Crystallographic structure of Li_2MnO_3

It is well known that the $[Mn_{2/3}Li_{1/3}]$ layers in Li_2MnO_3 form a $[\sqrt{3} \times \sqrt{3}]R30^\circ$-type superlattice. In contrast, the stacking sequence of the $[Mn_{2/3}Li_{1/3}]$ superlattice has not been clarified yet. Lang proposed three types of probable stacking sequence of AB_2 layers in rock-salt-related A_2BO_3 compounds, such as Li_2MnO_3 and Li_2SnO_3, corresponding to the space-group symmetries of $C2/m$, $C2/c$, and $P3_112$ (or $P3_212$) [23]. The structure refinement of Li_2MnO_3 has been reported using the space-group symmetry of $C2/m$ or $C2/c$ [24,25]. Recently, Meng and coworkers proposed a disordered model consisting of the $C2/m$ and $P3_112$ stacking sequences [26,27]. The effects of the stacking sequence on energy were confirmed before examining the lithium removal using the three models proposed by Lang.

The calculated energies of Li_2MnO_3 were similar for the three types of stacking sequence. The difference was within 0.001 eV per formula unit. This is consistent with the results of a first-principles pseudopotential calculation [27]. In addition to the similar energies, the crystallographic structures were also similar for the three stacking sequences. The calculated structural parameters of the $C2/m$ model are summarized in Table 1. The lattice constants were overestimated by 1–2% compared with the experimental results. This is a reasonable error for the use of GGA+U [15]. The ratio of b to a, 1.729, was almost the same as the ideal value for a hexagonal lattice, $\sqrt{3}$. The lattice vector $\boldsymbol{a+3c}$ in the model, which corresponds to the lattice vector $\boldsymbol{c}$ in the α-$NaFeO_2$-type structure, was almost normal (90.32°) to the a–b plane. Hence, the lattice can be regarded as hexagonal, even though its symmetry is monoclinic. The $C2/c$ model also has an almost hexagonal lattice. The lattice constants are, therefore, compared among the three models using the corresponding lattice constants of the α-$NaFeO_2$-type structure, as summarized in Table 2. The corresponding lattice constant a is estimated from the area of the a–b plane, and c is calculated from the interlayer distance of the $[Mn_{2/3}Li_{1/3}]$ layers. The differences were within the computational accuracy. The identical energy and lattice constants suggest a disordered stacking sequence, whereas a tendency of ordering was reported in the literature [26,27]. The cause of this inconsistency is not yet clear, but the stacking sequence appears to have little effect on the redox mechanism. The $C2/m$ model is therefore employed to examine the lithium removal.

Table 1
Structural parameters of Li_2MnO_3 with the $C2/m$-type stacking sequence

Atom	Site	x	y	z
Li (1)	2b	0	0.5	0
Li (2)	2c	0	0	0.5
Li (3)	4h	0	0.66115	0.5
Mn	4g	0	0.16706	0
O (1)	4i	0.21946	0	0.22822
O (2)	8j	0.25417	0.32145	0.22436

Space group: $C2/m$ (12), a = 5.0196 Å, b = 8.6763 Å, c = 5.0930 Å, β = 109.50°.

Table 2
Lattice constants of Li_2MnO_3 corresponding to the α-$NaFeO_2$-type structure

Stacking sequence	a (Å)	c (Å)
$C2/m$	2.8951	14.4022
$C2/c$	2.8949	14.4027
$P3_112$	2.8949	14.4027

a is calculated from the area of the a–b plane, and c is calculated from the interlayer distance of the $[Mn_{2/3}Li_{1/3}]$ layers.

3.2. Lithium removal from Li_2MnO_3

There have been several mechanisms proposed for the electrochemical activity of Li_2MnO_3 and its derivatives, as described in the introduction. A key question is whether the Li ions can be removed from Li_2MnO_3 at a potential of ∼4.5 V. A series of $Li_{2-x}MnO_3$ compounds were thus examined, assuming topotactic lithium removal. Since the primitive cell of the $C2/m$ model contains two formula units ($Li_4Mn_2O_6$), three compositions were considered: $Li_{1.5}MnO_3$ (the primitive cell of $Li_3Mn_2O_6$), $Li_{1.0}MnO_3$ ($Li_2Mn_2O_6$), and $Li_{0.5}MnO_3$ ($Li_1Mn_2O_6$). All possible arrangements of the Li ions and vacant sites within the primitive cell were examined.

There are three different sites for the Li ions in the $C2/m$ model, i.e., at Wyckoff positions of 2b, 2c, and 4h. The 2b site is in the $[Mn_{2/3}Li_{1/3}]$ layers, while the 2c and 4h sites are in the Li layers. Hence, three different arrangements were examined for $Li_{1.5}MnO_3$. The models with the Li vacancies in the Li layers exhibited similar energy; the difference was less than 0.01 eV per formula unit of $Li_{1.5}MnO_3$. In contrast, the other model, with the vacancies in the $[Mn_{2/3}Li_{1/3}]$ layers, was higher in energy by 0.07 eV per formula unit, suggesting the removal of lithium from the Li layers at the beginning of charging. The redox potential for the lithium removal can be approximately calculated as the average potential of Li_xMnO_3 in the range of x_1 to x_2 by the following equation:

$$V_{\mathrm{ave}}(x_1 \le x \le x_2) = -\frac{E[\mathrm{Li}_{x_2}\mathrm{MnO}_3] - E[\mathrm{Li}_{x_1}\mathrm{MnO}_3] - (x_2 - x_1)E[\mathrm{Li}]}{(x_2 - x_1)e},$$

where $E[X]$ is energy of X per formula unit and e is the elementary charge. Entropy, volume change, and temperature effects are ignored. The average potential was estimated to be 4.60 V for lithium removal from the Li layers. This value was close to the potential of the plateau observed in the first charging of Li_2MnO_3 and its derivatives.

The density of states (DOS) was calculated to discuss the charge compensation mechanism for the lithium removal. The DOS of Li_2MnO_3 and $Li_{1.5}MnO_3$ with the most stable arrangement are illustrated in Fig. 1. In Li_2MnO_3, Mn-3d states were split into the so-called t_{2g} and e_g bands, and only the t_{2g} band in the spin-up state was filled. This is the typical electronic structure of the Mn^{4+} ion at octahedral sites. The electronic structure of Mn was not significantly changed upon the lithium removal. The top states of Li_2MnO_3 were mainly contributed to by oxygen. Hence, the charge compensation for the lithium removal was predominantly carried out by the oxidation of oxygen.

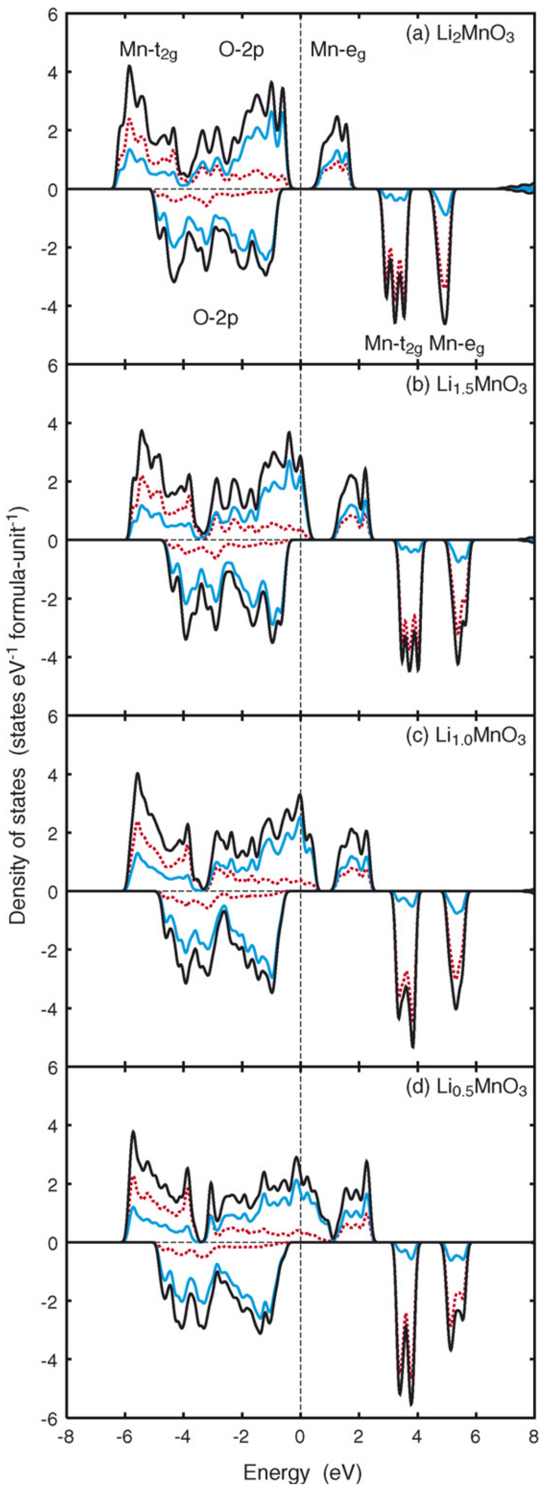

Fig. 1. Density of states of Li_xMnO_3 ($x = 2$, 1.5, 1 and 0.5) for the most stable arrangements of Li ions. The density of states is aligned so that the Fermi energy is zero. The projected density of states for Mn and O is illustrated by red-broken and blue-solid lines, respectively.

There are four different arrangements of the Li ions in $Li_{1.0}MnO_3$: two have Li vacancies in the Li layers only, and the other two have Li vacancies in both the Li and $[Mn_{2/3}Li_{1/3}]$ layers. It was possible to classify the energy of the four models by considering the arrangements. The two models with Li vacancies in both the Li and $[Mn_{2/3}Li_{1/3}]$ layers exhibited a lower energy by ∼0.06 eV per formula unit than the other two models with Li vacancies in the Li layers only. The difference in energy was less than 0.02 eV per formula unit among each pair. The results indicate that the Li ions in the $[Mn_{2/3}Li_{1/3}]$ layers are likely to be removed from $Li_{1.5}MnO_3$ to form $Li_{1.0}MnO_3$. The calculated potential required to remove the Li ions in the $[Mn_{2/3}Li_{1/3}]$ layers ranged from 4.56 to 4.61 V. The variation of the potential was due to the arrangement of the Li ions in the Li layers. The potential from $Li_{1.5}MnO_3$ to $Li_{1.0}MnO_3$ was slightly lower than that from Li_2MnO_3 to $Li_{1.5}MnO_3$. This means that $Li_{1.5}MnO_3$ is metastable, although the difference in energy between $Li_{1.5}MnO_3$ and the pair of Li_2MnO_3 and $Li_{1.0}MnO_3$ was small. Consideration of the effects of entropy, volume changes, and temperature, which have been disregarded in this study, would be necessary for further discussion on whether the redox reaction occurs through a single phase or two phases. Assuming a two-phase redox reaction, the estimated average potential from Li_2MnO_3 to $Li_{1.0}MnO_3$ is 4.58 V. The DOS of $Li_{1.0}MnO_3$ with the most stable arrangement is illustrated in Fig. 1. The top valence states were predominantly contributed to by oxygen, as before, indicating the charge compensation by oxygen.

Three different arrangements of the Li ions were considered for $Li_{0.5}MnO_3$. Since the Li ions in the $[Mn_{2/3}Li_{1/3}]$ layers have been already removed in $Li_{1.0}MnO_3$ with the most stable arrangement, it would be reasonable to expect that the Li ions are stably located in the Li layers in $Li_{0.5}MnO_3$. The model with the Li ions at the 2c site, however, exhibited only 0.03 eV per formula unit lower energy than that with the Li ions at the 2b site. The difference in the potential energy of the Li site between the Li and $[Mn_{2/3}Li_{1/3}]$ layers was much smaller than those in $Li_{1.5}MnO_3$ and $Li_{1.0}MnO_3$. The redox potential for the lithium removal from the Li layers was estimated to be 4.65 V, slightly higher than that from Li_2MnO_3 to $Li_{1.0}MnO_3$. The DOS of $Li_{0.5}MnO_3$ with the Li ions at the 2c site is illustrated in Fig. 1 and indicates that the charge was still compensated by oxygen. Interestingly, the model with the Li ions at half of the 4h site eventually transformed into an O1-type stacking sequence during the geometry optimization calculation. The obtained structure was that of $PbSb_2O_6$ with a space-group symmetry of $P\bar{3}1m$. The O1-type model was lower in energy than the model with the Li ions at the 2c site by 0.31 eV per formula unit of $Li_{0.5}MnO_3$. The transformation is expected to be irreversible because of the large change in energy.

The calculation results of this study suggest that the Li ion can be removed from Li_2MnO_3 at a potential of ∼4.6 V with a wide plateau. This is in good agreement with the characteristic profile during the first charging of Li_2MnO_3 and its derivatives. Oxygen predominantly contributes to the charge compensation associated with the lithium removal. It would be necessary to take account of the kinetics and environment, such as temperature and oxygen pressure, for further discussion on which reaction occurs following the lithium removal.

4. Conclusions

The effects of the stacking sequence of the $[Mn_{2/3}Li_{1/3}]$ layers of Li_2MnO_3 on its energy and crystallographic structure were examined. The difference in energy was small among the three models with the $C2/m$, $C2/c$ and $P3_112$-type stacking sequences. The lattice constants were equal among the three models. The energy and lattice constants suggest a disordered stacking sequence of the $[Mn_{2/3}Li_{1/3}]$ layers in Li_2MnO_3. The systematic calculation for $Li_{2-x}MnO_3$ with a variety of arrangements of Li ions suggests that lithium removal occurs at ∼4.6 V with a wide potential plateau. The electronic structure indicates that the charge compensation associated with lithium removal is performed by the oxidation of oxygen.

References

[1] K. Numata, C. Sakaki, S. Yamanaka, Chem. Lett. (1997) 725.
[2] K. Numata, C. Sakaki, S. Yamanaka, Solid State Ionics 117 (1999) 257.
[3] B. Ammundsen, J. Paulsen, I. Davidson, R.-S. Liu, C.-H. Shen, J.-M. Chen, L.-Y. Jang, J.-F. Lee, J. Electrochem. Soc. 149 (2002) A431.
[4] M. Tabuchi, A. Nakashima, H. Shigemura, K. Ado, H. Kobayashi, H. Sakaebe, H. Kageyama, T. Nakamura, M. Kohzaki, A. Hirano, R. Kanno, J. Electrochem. Soc. 149 (2002) A509.
[5] Z. Lu, J.R. Dahn, J. Electrochem. Soc. 149 (2002) A815.
[6] A.D. Robertson, P.G. Bruce, Chem. Commun. 23 (2002) 2790.
[7] A.D. Robertson, P.G. Bruce, Chem. Mater. 15 (2003) 1984.
[8] J.-S. Kim, C.S. Johnson, J.T. Vaughey, M.M. Thackeray, S.A. Hackney, W.-S. Yoon, C.P. Grey, Chem. Mater. 16 (2004) 1996.
[9] C.S. Johnson, J.-S. Kim, C. Lefief, N. Li, J.T. Vaughey, M.M. Thackeray, Electrochem. Commun. 6 (2004) 1085.
[10] D. Pasero, V. McLaren, S. de Souza, A.R. West, Chem. Mater. 17 (2005) 345.
[11] M.K. Aydinol, A.F. Kohan, G. Ceder, K. Cho, J. Joannopoulos, Phys. Rev. B 56 (1997) 1354.
[12] C. Wolverton, A. Zunger, Phys. Rev. B 57 (1998) 2242.
[13] A. Van der Ven, G. Ceder, Electrochem. Solid-State Lett. 3 (2000) 301.
[14] Y. Koyama, I. Tanaka, H. Adachi, Y. Uchimoto, M. Wakihara, J. Electrochem. Soc. 150 (2003) A63.
[15] F. Zhou, M. Cococcioni, C.A. Marianetti, D. Morgan, G. Ceder, Phys. Rev. B 70 (2004) 235121.
[16] J.P. Perdew, K. Burke, M. Ernzerhof, Phys. Rev. Lett. 78 (1997) 1396.
[17] S.L. Dudarev, G.A. Botton, S.Y. Savrasov, C.J. Humphreys, A.P. Sutton, Phys. Rev. B 57 (1998) 1505.
[18] P.E. Blöchl, Phys. Rev. B 50 (1994) 17953.
[19] G. Kresse, J. Hafner, Phys. Rev. B 47 (1993) R558.
[20] G. Kresse, J. Furthmüller, Phys. Rev. B 54 (1996) 11169.
[21] G. Kresse, D. Joubert, Phys. Rev. B 59 (1999) 1758.
[22] H.J. Monkhorst, J.D. Pack, Phys. Rev. B 13 (1976) 5188.
[23] G. Lang, Z. Anorg. Allg. Chem. 348 (1966) 246.
[24] P. Strobel, B. Lambert-Andron, J. Solid State Chem. 75 (1988) 90.
[25] A. Riou, A. Lecerf, Y. Gerault, Y. Cudennec, Mater. Res. Bull. 27 (1992) 269.
[26] Y.S. Meng, G. Ceder, C.P. Grey, W.-S. Yoon, M. Jiang, J. Bréger, Y. Shao-Horn, Chem. Mater. 17 (2005) 2386.
[27] J. Bréger, M. Jiang, N. Dupré, Y.S. Meng, Y. Shao-Horn, G. Ceder, C.P. Grey, J. Solid State Chem. 178 (2005) 2575.